Integrative Cancer Therapies
Volume 23: 1–21

DOI: 10.1177/15347354241237973
journals.sagepub.com/home/ict
Sage

Clinical Efficacy and Gut Microbiota Regulating-Related Effect of Si-Jun-Zi Decoction in Postoperative Non-Small Cell Lung Cancer Patients: A Prospective Observational Study

Yiyun He, MD[1], Ao Qi, PhD[1], Yifeng Gu, MD[1], Congmeng Zhang, MM[1], Yichao Wang, MD[1], Wenxiao Yang, PhD[1], Ling Bi, PhD[1], Yabin Gong, MD[1], Lijing Jiao, PhD[1], and Ling Xu, PhD[1]

Abstract

Background: Postoperative non-small cell lung cancer (NSCLC) patients frequently encounter a deteriorated quality of life (QOL), disturbed immune response, and disordered homeostasis. Si-Jun-Zi Decoction (SJZD), a well-known traditional Chinese herbal formula, is frequently employed in clinical application for many years. Exploration is underway to investigate the potential therapeutic effect of SJZD for treating postoperative NSCLC. **Objective:** To assess the efficacy of SJZD on QOLs, hematological parameters, and regulations of gut microbiota in postoperative NSCLC patients. **Methods:** A prospective observational cohort study was conducted, enrolling 65 postoperative NSCLC patients between May 10, 2020 and March 15, 2021 in Yueyang Hospital, with 33 patients in SJZD group and 32 patients in control (CON) group. The SJZD group comprised of patients who received standard treatments and the SJZD decoction, while the CON group consisted of those only underwent standard treatments. The treatment period was 4 weeks. The primary outcome was QOL. The secondary outcomes involved serum immune cell and inflammation factor levels, safety, and alterations in gut microbiota. **Results:** SJZD group showed significant enhancements in cognitive functioning ($P = .048$) at week 1 and physical functioning ($P = .019$) at week 4. Lung cancer-specific symptoms included dyspnea ($P = .001$), coughing ($P = .008$), hemoptysis ($P = .034$), peripheral neuropathy ($P = .019$), and pain (arm or shoulder, $P = .020$, other parts, $P = .019$) eased significantly in the fourth week. Anemia indicators such as red blood cell count ($P = .003$ at week 1, $P = .029$ at week 4) and hemoglobin ($P = .016$ at week 1, $P = .048$ at week 4) were significantly elevated by SJZD. SJZD upregulated blood cell cluster differentiation (CD)3^+ ($P = .001$ at week 1, $P < .001$ at week 4), $CD3^+CD4^+$ ($P = .012$ at week 1), $CD3^+CD8^+$ ($P = .027$ at week 1), $CD19^+$ ($P = .003$ at week 4), increased anti-inflammatory interleukin (IL)-10 ($P = .004$ at week 1, $P = .003$ at week 4), and decreased pro-inflammatory IL-8 ($P = .004$ at week 1, $p = .005$ at week 4). Analysis of gut microbiota indicated that SJZD had a significant impact on increasing microbial abundance and diversity, enriching probiotic microbes, and regulating microbial biological functions. **Conclusions:** SJZD appears to be an effective and safe treatment for postoperative NSCLC patients. As a preliminary observational study, this study provides a foundation for further research.

Keywords
postoperative lung cancer, non-small cell lung cancer, gut microbiota, quality of life, Si-Jun-Zi decoction

Submitted September 13, 2023; revised February 7, 2024; accepted February 22, 2024

Introduction

Globally, lung cancer stands as the primary contributor to cancer-related mortality.[1] Following surgery, individuals diagnosed with non-small cell lung cancer (NSCLC) frequently encounter a worse quality of life (QOL),[2] compromised nutritional health,[3] impaired immune functions, and inflammatory responses,[4] which disrupt the equilibrium of the body and impede daily activities. The conceptual framework underlying enhanced recovery after surgery (ERAS) has transitioned from stress avoidance to prioritizing the preservation of perioperative homeostasis in patients, with the core being to maintain the balance of the patient's perioperative internal environment.[5-7] Maintaining intestinal

homeostasis is a crucial component of perioperative equilibrium, encompassing volume and electrolyte balance, gut microbiota composition, and internal environment.[8-10] The presence of gut bacteria is strongly linked to detrimental effects on the mucosal barrier of intestines,[11] the translocation of microflora,[12] and the regulation of metabolism,[13] leading to immune microenvironment disorders and chronic inflammation.[14] Dysbiosis in the intestinal flora can disrupt the gut-lung axis by suppressing immune functions, producing proinflammatory substances, and modulating metabolic pathways.[15] Thus, managing the gut microbiome as a novel adjunctive treatment modality for postoperative NSCLC could be considered.

The Si-Jun-Zi Decoction (SJZD), a renowned traditional Chinese medicine (TCM) prescription documented in the Prescriptions of Peaceful Benevolent Dispensary (Tai Ping Hui Min He Ji Ju Fang) during the Song Dynasty, exhibits effectiveness in enhancing vitality and optimizing the functioning of the spleen. The composition of SJZD consists of 4 botanical constituents: Ginseng Radix et Rhizoma (Renshen), Rhizoma Atractylodis Macrocephalae (Baizhu), Poria cocos (Fuling), and Glycyrrhizae Radix et Rhizoma (Gancao). The constituents and primary bioactive compounds of SJZD have been investigated deeply.[16-18] Furthermore, the pharmacokinetic properties and pharmacodynamic material foundations of SJZD have also been comprehensively elucidated.[19] SJZD is extensively employed in clinical practice for patients exhibiting vital energy deficiency, displaying satisfactory efficacy and safety, in addition, SJZD has garnered recognition for its potential in managing lung cancer by impeding tumor occurrence and progression.[20-23] SJZD demonstrates effectiveness in treating gastrointestinal diseases and spleen-deficiency syndrome, ameliorating gastrointestinal dysfunction, enhancing malnutrition state, and promoting performance status.[24] In addition to its ability to protect the intestinal mucosal restitution,[25] SJZD also enhances intestinal immunity,[26] alleviates mucositis, and maintains intestinal homeostasis.[27]

However, it is still unknown whether SJZD intervention would lead to better therapeutic outcomes in the treatment of postoperative NSCLC. Based on the regulation of intestinal homeostasis and the antitumor effect demonstrated by SJZD, it is hypothesized that SJZD may exert an influence on the lung-gut axis through its impact on the regulation of intestinal microbiota. This, in turn, may contribute to the restoration of the equilibrium of the internal environment in human body and expedite the postoperative recovery of lung cancer. Hence, a prospective observational cohort study was carried out to assess the effectiveness and safety of SJZD in postoperative NSCLC patients, encompassing evaluations of QOL, changes in hematological parameters, and alterations in gut microbiota.

Methods

Study Design

The prospective observational cohort study assessed the efficacy of SJZD in comparison to standard therapy among patients with postoperative NSCLC at Yueyang Hospital of Integrated Traditional Chinese and Western Medicine affiliated to Shanghai University of TCM (Shanghai, China) (referred to as Yueyang Hospital). The primary outcome was the assessment of QOL. The secondary outcomes included the evaluation of changes in serum immune cells and inflammation factors level, alterations in gut microbiota and the assessment of safety. The study was conducted in conformity to the World Medical Association declaration of Helsinki and was approved by the Ethics Committee of Yueyang Hospital (No. 2020-038). Prior to their participants in the study, all patients provided written informed consent.

Participants

Participants were included according to the following inclusion criteria: (1) Individuals diagnosed with NSCLC through histological or pathological examination within 7 days after surgery; (2) Aged between 18 and 74 years; (3) Patients who remained clinically stable after the surgery; (4) Karnofsky Performance Status (KPS) scores ≥ 60; (5) With informed consent. Patients were excluded if they were: (1) With serious chronic diseases such as severe cardiac, cerebrovascular, respiratory, hepatic, renal, and immune diseases; (2) Having the history of other malignant tumors or the digestive surgery within the past 5 years; (3) With serious infectious diseases like bacterial pneumonia,

[1]Department of Oncology, Yueyang Hospital of Integrated Traditional Chinese and Western Medicine, Shanghai University of Traditional Chinese Medicine,Shanghai , China

Corresponding Authors:
Ling Xu, Department of Oncology, Yueyang Hospital of Integrated Traditional Chinese and Western Medicine, Shanghai University of Traditional Chinese Medicine, No. 110, Ganhe Road, Hongkou District, Shanghai 200437, China.
Email: xulq67@shutcm.edu.cn

Lijing Jiao, Department of Oncology, Yueyang Hospital of Integrated Traditional Chinese and Western Medicine, Shanghai University of Traditional Chinese Medicine, No. 110, Ganhe Road, Hongkou District, Shanghai 200437, China.
Email: jiaolijing@shyueyanghospital.com

gastrointestinal inflammation, or others within the past 3 months; (4) Taking corticosteroids, non-steroidal anti-inflammatory drugs; (5) Taking microbial agents such as probiotics or synbiotics within 1 month. The diagnostic standards for NSCLC adhered to the 2018 edition of the Chinese Guidelines on the Diagnosis and Treatment of Primary Lung Cancer issued by the National Health Commission of the People's Republic of China, as well as the eighth edition of the American Joint Committee on Cancer (AJCC) TNM staging system.

Procedures

The study recruited patients with NSCLC who had undergone surgery. The allocation of columns was based on the patients' willingness to receive TCM. The CON group received standard supportive treatment, while the SJZD group received a combination of SJZD and standard supportive treatment. The standard supportive treatment included the administration of antitussive, expectorant, hemostasis, or other appropriate treatments to relieve postoperative symptoms such as cough, expectoration, and hemoptysis. The administration of these treatments followed the guidelines specified in the 2019 edition of the Chinese Expert Consensus on Perioperative Lung Protection in Thoracic Surgery and the 2020 edition of the Chinese Guidelines for Perioperative Airway Management in Thoracic Surgery.

In the SJZD group, a decoction of SJZD was administered, comprising 4 types of herbs: Ginseng Radix et Rhizoma (15 g), Rhizoma Atractylodis Macrocephalae (9 g), Poria cocos (15 g), and Glycyrrhizae Radix et Rhizoma (6 g). The decoction was prepared by the TCM Pharmacy of Yueyang Hospital following a standardized production process. The SJZD medicinal materials were authorized and manufactured in compliance with good manufacturing practice (GMP) standards by the Bureau of National Health Insurance. Patients were directed to take 200ml of the decoction twice a day (at 9:00 AM and 14:00 PM) for a period of 4 weeks, unless they encountered unbearable adverse reactions.

Clinical Outcomes and Instruments

The primary outcome was the clinical remission of QOL, referring to the least-squares (LS) mean changes in QOL from the baseline to week 1 and week 4. The secondary outcomes included evaluating changes in serum immune cell and inflammation factor levels, safety assessments, and alterations in gut microbiota.

The European Organization for Research and Treatment of Cancer (EORTC) Quality of Life Questionnaire Core 30 (QLQ-C30) (Version 3.0) and the Quality of Life Questionnaire Lung Cancer Module 13 (QLQ-LC13) were utilized to assess QOL.[28,29] Standardization of the scales and item scores of QLQ-C30 and QLQ-LC13 was achieved through a linear transformation, yielding a scale ranging from 0 to 100. Higher scores on functioning scales or global health status/quality of life (GHS/QOL) score indicate an improved health status, whereas higher scores on symptom scales reflect a greater severity of symptoms. Professionals who received training conducted this study to assess the QOL using the QLQ-C30 and QLQ-LC13 surveys.

Flow cytometry (FCM) was used to test immunity indices such as blood cell cluster differentiation (CD) antigens including $CD3^+$, $CD4^+$, $CD8^+$, $CD3^+CD4^+$, $CD3^+CD8^+$, $CD4^+/CD8^+$, $CD56^+$. Enzyme-linked immunosorbent assay (ELISA) was employed to examine cytokines associated with inflammation, including interleukin (IL)-1β, IL-2 receptor, IL-6, IL-8, IL-10, and tumor necrosis factor (TNF)-α. Routine blood and biochemical examinations were conducted to assess safety. The laboratory indicators mentioned above were tested at 3 specific time points (baseline, week 1, and week 4) by the clinical laboratory of Yueyang Hospital.

Fecal samples were collected prior to the treatments, at week 1, and at week 4, using the MGIEasy kit (MGI Tech Co., Ltd. China), and following the standard operating procedures.[30,31] The analysis of gut microbiota and functional predictions was conducted through DNA extraction, polymerase chain reaction (PCR) amplification, and Illumina MiSeq sequencing, employing 16S Ribosomal RNA (16S rRNA) gene sequencing. The Miseq libraries, known as Illumina sequencing libraries, were created by following the established Illumina library preparation protocol using the NEXTFLEX Rapid DNA-Seq Kit (Bioo Scientific, the United States). The Illumina Miseq PE300 platform (Illumina, the United States) was used for high-throughput sequencing.

Safety assessments included the observation of adverse events (AEs), vital signs, clinical laboratory examinations, and physical examinations. The documentation of any AEs, including toxicity and side effects, adhered to the guidelines in the Common Terminology Criteria for Adverse Events (CTCAE Version 5.0) set forth by the National Cancer Institute.

Statistical Analysis

Sample size. The determination of the sample size and statistical power was based on the distributions of the measurement index, rarefaction curves, and microbial diversity observed in a previously published study. Phylogenetic diversity (PD) is one of the various metrics used to assess alpha diversity. Based on the standard calculation for determining sample size, a total of 50 patients can be deemed satisfactory to attain an adequate statistical power ($1-\beta = 80\%$) for a mean difference of 3 PD units of the effect

size, which is equivalent to an effect size of Cohen's D of approximately 0.82.[32,33] Given the prevalence of constipation among postoperative patients and the need for rigorous quality control of fecal samples, a final dropout rate of 30% was deemed appropriate, surpassing the typical rate of 20%. Consequently, the sample size was ultimately established at 65 patients.

Microbiome bioinformatics analysis. The quality control of the raw sequences was performed using the Fastp software (https://github.com/OpenGene/fastp, Version 0.20.0).[34] After performing chimera check, the sequences underwent quality filtering and were subsequently merged using FLASH software (http://www.cbcb.umd.edu/software/flash, Version 1.2.7).[35] QIIME (Version 1.8.0) was used to cluster the high-grade sequence reads into Operational Taxonomic Units (OTUs) based on a 97% similarity threshold. The chimera was eliminated utilizing the Usearch algorithm from QIIME (Version 1.8.0) resulting in the acquisition of OTU representative sequences. In the taxonomic analysis, the Ribosomal Database Project (RDP) classifier (http://rdp.cme.msu.edu/, Version 2.2) was employed to annotate each sequence for species classification.[36] The annotated sequences were then compared to the Greengenes 2013-08 release database (http://greengenes.lbl.gov/Download/). The threshold of comparison to 80% was set for each OTU taxonomic information.

Alpha diversity, which represents the richness and uniformity within a community, was assessed using various calculations including the Chao index, Sobs index, Shannon index, Simpson index, rarefaction curve, and rank-abundance curve.[37,38] Principal Coordinate Analysis (PCoA) based on unweighted UniFrac was performed to analyze Beta diversity, which quantifies the diversity between communities.[39] ANOSIM was utilized to calculate the statistical significance through analysis of similarities. The Linear Discriminant Analysis (LDA) Effect Size (LEfSe) method was employed to detect potential microbial biomarkers that exhibited significant statistical differences at various levels.[40] The effect size of the corresponding differential species abundance is evaluated using LDA after LEfSe undergoes a non-parametric factorial Kruskal-Wallis (KW) rank sum test. In this study, the logarithmic LDA score was considered to be significant if it exceeded 2.0 and P-value $< .05$ (determined by factorial KW test). To analyze the co-occurrence networks, Spearman correlations were calculated using the R package "Hmisc." The Spearman's rank correlation coefficient (ρ) was utilized to calculate the pairwise correlations among the abundances of the bacterial genera. To correct multiple test P-values, the Benjamini-Hochberg (FDR-BH) method was used to calculate the adjusted P-values. It was constructed a co-occurrence network with a significant correlation ($|\rho| \geq .6$, adjust $P < .01$) by the R package "igraph." The construction of the co-occurrence network of gut microbiota was visualized using Gephi (Version 0.9.4). Functional enrichment variations were determined by conducting the functional predictions of gut microbiota in Kyoto Encyclopedia of Genes and Genomes (KEGG) pathways using Phylogenetic Investigation of Communities by Reconstruction of Unobserved States 2 (PICRUSt2) (https://github.com/picrust/picrust2).[41-43]

Statistical methods. The clinical features, including dichotomous or categorical variables, were presented as absolute numbers or percentages. Continuous variables were represented as means ± standard error of mean (SEM) or as medians with interquartile range (IQR). In order to evaluate the differences in measurement data between 2 groups, the independent sample T-test or the Wilcoxon Mann-Whitney U rank sum test was used for measurement data. Count data, such as gender, were compared using the Chi-square test. The Wilcoxon Mann-Whitney U rank sum test was used for ranked data. All hypothesis tests were conducted using 2-sided tests and a 95% confidence interval (CI). Statistical significance was determined when the $P < .05$. In the case of multiple tests, P-values were adjusted using the FDR-BH method by Benjamini-Hochberg. All statistical analyses were conducted using SPSS Statistics software (Version 22.0; IBM Corp).

Results

Characteristics of patients

From May 10, 2020 to March 15, 2021, a total of 65 eligible postoperative NSCLC patients were enrolled in the prospective observational study (Figure 1).

All subjects received questionnaires before and 1 week after treatment. Of the 65 patients recruited, 31/33 (93.94%) in the SJZD group and 29/32 (90.63%) in the CON group completed the QOL assessment at week 4. Part of the questionnaire was incomplete due to patient noncompliance. Regarding immunity and inflammation-related cytokines, all participants completed the baseline assessment, 95.38% (SJZD group: 33 patients, CON group: 29 patients) completed the assessment at week 1, and 87.69% (SJZD group: 31 patients, CON group:26 patients) completed the assessment at week 4. The most common reason for missing blood samples was attributed to missing the designated time frame or patients' refusal. In terms of the fecal sample collection, of the 65 patients recruited, 83.08% (SJZD group: 32 patients, CON group: 22 patients) successfully completed the baseline assessment, 56.92% (SJZD group: 22 patients, CON group: 15 patients) completed week 1, and ultimately, 47.69% (SJZD group: 22 patients, CON group: 9 patients) completed week 4. Missing fecal samples were mainly attributed to constipation or being excluded due to poor

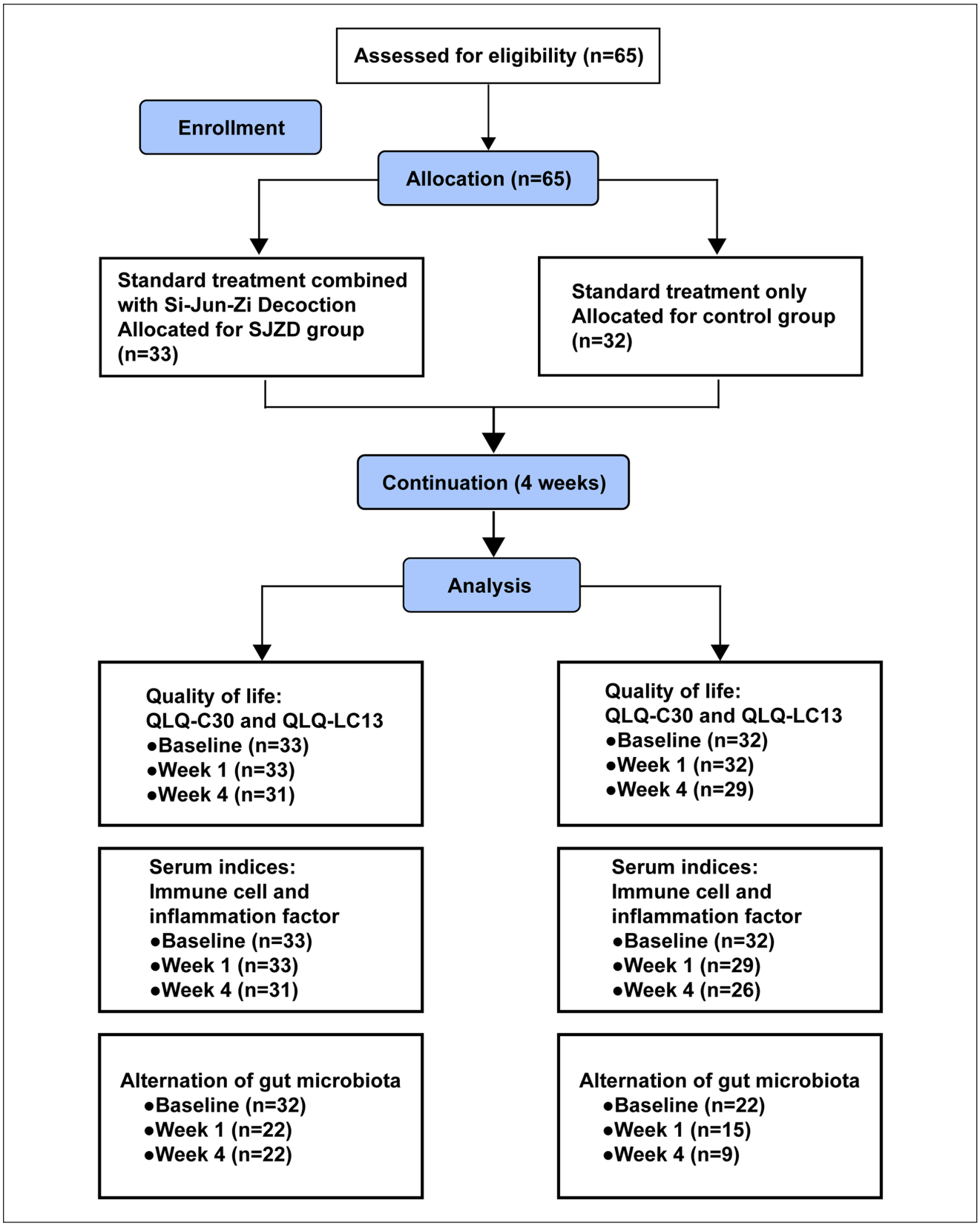

Figure 1. The flow diagram of the study.

Table 1. Baseline Characteristics of Postoperative NSCLC Patients.

Variables	SJZD group (n = 33)	CON group (n = 32)	Statistics t/Z/χ^2	*P*
Age, years, Mean ± SD	59.24 ± 12.23	59.73 ± 10.22	−0.062	.951
Gender, n (%)			2.747	.097
Male	17 (51.52)	10 (31.25)		
Female	16 (48.48)	22 (68.75)		
Smoking status, n (%)			0.337	.562
Smoker	7 (21.21)	5 (15.63)		
Nonsmoker	26 (78.79)	27 (84.37)		
Cancer family history, n (%)			0.085	.771
Yes	6 (18.18)	5 (15.63)		
No	27 (81.82)	27 (84.37)		
Pathological types, n (%)			1.225	.742
Adenocarcinoma	32 (96.97)	30 (93.75)		
Squamous cell carcinoma	1 (3.03)	1 (3.125)		
Adenosquamous carcinoma	0 (0.00)	1 (3.125)		
TNM stage, n (%)			1.871	1.000
Ia	32 (96.97)	31 (96.88)		
Ib	1 (3.03)	0 (0.00)		
IIa	0 (0.00)	1 (3.12)		
Mode of surgical procedure, n (%)			1.010	.603
Pulmonarylobectomy	26 (78.79)	22 (68.75)		
Segmentectomy	5 (15.15)	8 (25.00)		
Pulmonary wedge resection	2 (6.06)	2 (6.25)		
Thoracic drainage tube, n (%)			2.973	.085
Yes	15 (45.45)	8 (25.00)		
No	18 (54.55)	24 (75.00)		

quality control. There was a well-balanced characteristic distribution between 2 groups (Table 1).

Outcomes of Quality of Life (QOL)

At week 1, cognitive functioning was higher in the SJZD group than the baseline (LS mean change 5.05; 95% CI −0.17 to 10.27), whereas the CON group experienced a decline (LS mean change −1.04; 95% CI −5.61 to 3.52) ($P = .048$) (Figure 2A). At week 4, the SJZD group showed significantly greater improvements (LS mean change 17.63; 95% CI 9.99 to 25.28) in QLQ-C30 physical functioning compared to the CON group (LS mean change 5.52; 95% CI −1.33 to 12.36) ($P = .019$) (Figure 2B). Mean GHS/QOL scores compared with baseline were improved by 18.82 ± 32.56 points (95% CI 6.87 to 30.76) in SJZD group and 10.06 ± 31.84 points (95% CI −2.05 to 22.17) in CON group ($P = .297$).

Besides, at week 4, SJZD showed greater improvement compared to the CON group in dyspnea (LS mean change 36.92 [95% CI 27.84 to 45.99] improvement vs 16.86 [95% CI 9.31 to 24.40] improvement, $P = .001$), coughing (LS mean change 36.56 [95% CI 23.79 to 49.33] improvement vs 16.09 [95% CI 6.74 to 25.45] improvement, $P = .008$), hemoptysis (LS mean change 20.43 [95% CI 11.68 to 29.18] improvement vs 8.05 [95% CI 0.73 to 15.36] improvement, $P = .034$), peripheral neuropathy (LS mean change 4.30 [95% CI −1.81 to 10.41] improvement vs 6.90 [95% CI −0.19 to 13.99] deterioration, $P = .019$), pain (arm or shoulder) (LS mean change 20.43 [95% CI 12.27 to 28.59] improvement vs 5.75 [95% CI −3.26 to 14.76] improvement, $P = .020$), and pain (other parts) (LS mean change 15.05 [95% CI 6.22 to 23.89] improvement vs 0.00 [95% CI −8.30 to 8.30] improvement, $P = .019$) according to QLQ-LC13 (Figure 2F). Furthermore, there were no notable adverse effects of symptoms, indicating that SJZD exhibited a favorable safety profile. These results demonstrated that SJZD could improve the QOL by enhancing body function and ameliorating the discomfort symptoms with a good safety in postoperative NSCLC patients.

Clinical Serum Parameters

Routine blood and biochemical examinations. Routine blood testing and biochemical testing (liver and kidney functions) were analyzed to evaluate patients' general conditions (Figure 3A). SJZD had a notable impact on the elevation of red blood cell count (Week 1: $P = .003$, Week 4: $P = .029$) and hemoglobin (Week 1: $P = .016$, Week 4: $P = .048$) levels during both the first and fourth weeks. Hepatic function is

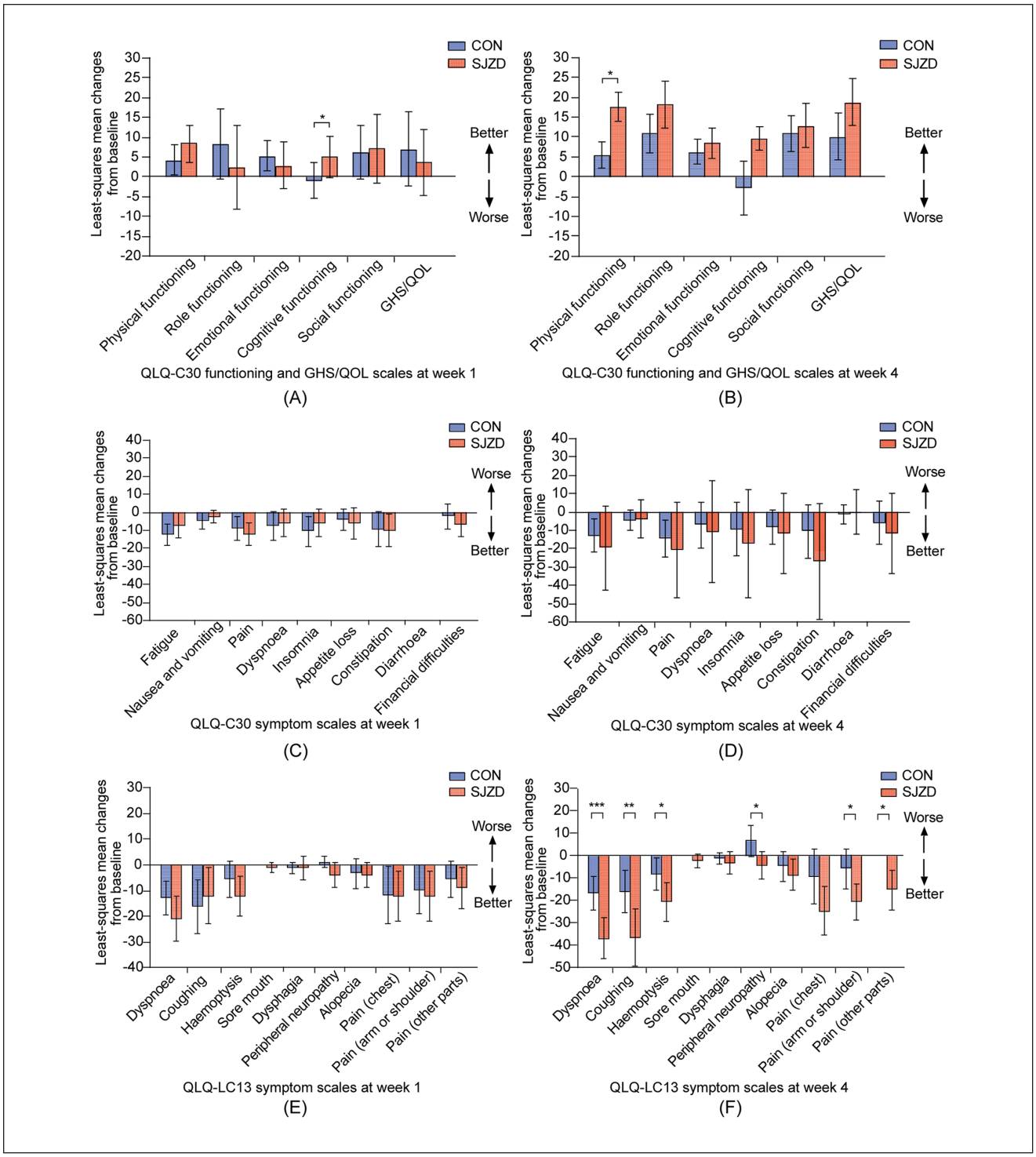

Figure 2. Mean changes from baseline to week 1 and week 4 for QLQ-C30 and QLQ-LC13 scales: (A) changes in QLQ-C30 functioning and GHS/QOL scales from baseline to week 1, (B) changes in QLQ-C30 functioning and GHS/QOL scales from baseline to week 4, (C) changes in QLQ-C30 symptom scales from baseline to week 1, (D) changes in QLQ-C30 symptom scales from baseline to week 4, (E) changes in QLQ-LC13 symptom scales from baseline to week 1, and (F) changes in QLQ-LC13 symptom scales from baseline to week 4. Error bars indicate 95% CIs around the mean. For the functioning and GHS/QOL scales, higher scores denote better QOL, while for the symptom scales, higher scores represent worse symptoms. EORTC QLQ-C30: European Organization for the Research and Treatment of Cancer Quality of Life Questionnaire Core 30 items. QLQ-LC30: Quality of Life Questionnaire Lung Cancer 13 items. GHS/QOL: global health status/quality of life. *$P < .05$. **$P < .01$. ***$P < .001$.

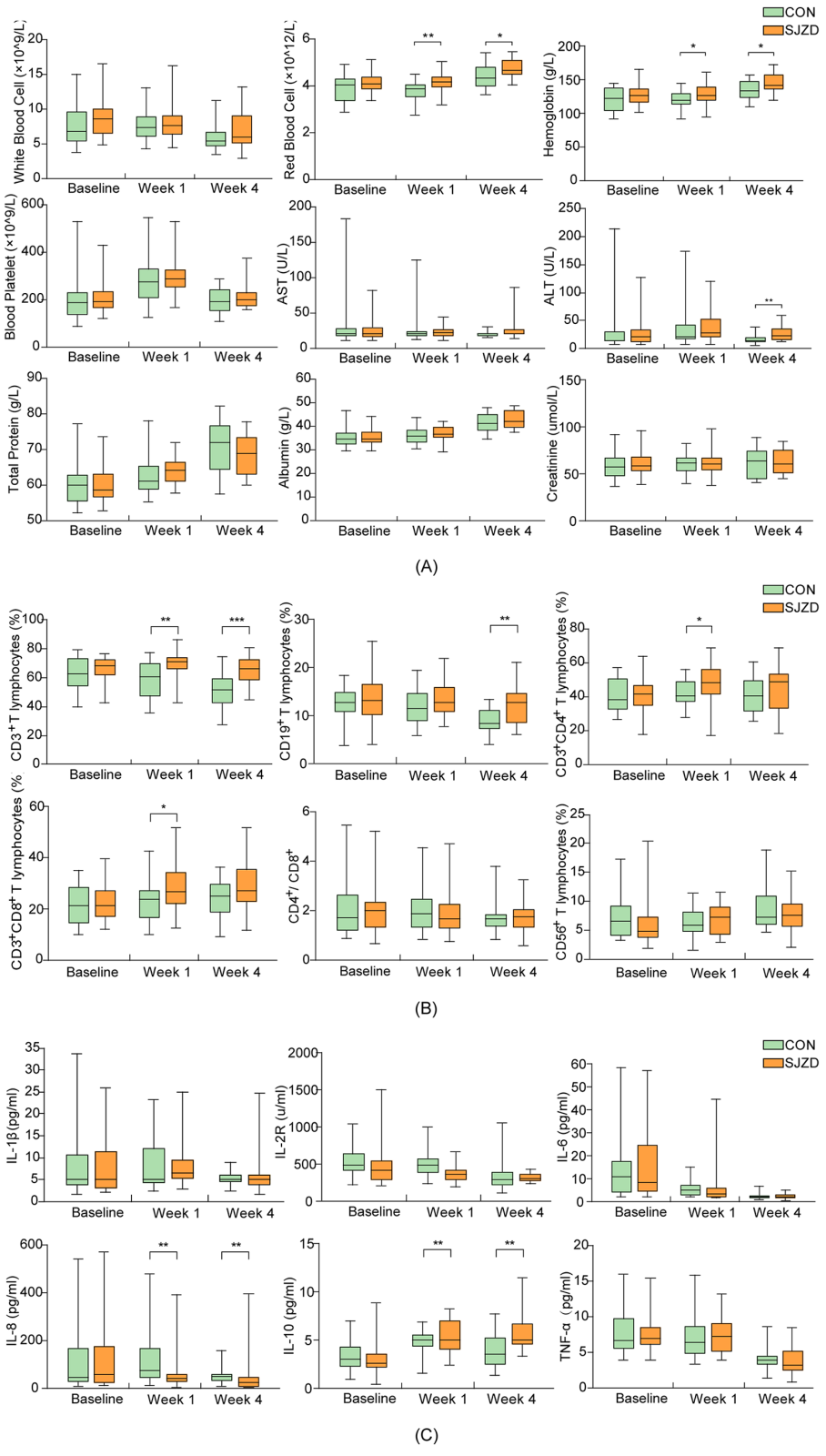

Figure 3. Routine blood, biochemical testing, immune function indices, and inflammatory-related cytokines in the SJZD and CON. (A) Routine blood, and biochemical testing. AST = Aspartate aminotransferase (U/L). ALT = Alanine aminotransferase (U/L). (B) Immune function index. (C) Inflammatory-related cytokines. *$P < .05$. **$P < .01$. ***$P < .001$.

associated with Aspartate aminotransferase (AST), Alanine aminotransferase (ALT), total protein, and albumin, while renal function is associated with creatinine. Despite the higher ALT level in SJZD group compared to the CON group ($P = .008$) after 4 weeks, the average ALT level remained within the normal range. No adverse effects related to blood routine examination, hepatic and renal function were observed.

Immune function indices. Following 1 week of treatment, the SJZD group demonstrated significantly increased levels of $CD3^+$ ($P = .001$), $CD3^+CD4^+$ ($P = .012$), and $CD3^+CD8^+$ ($P = .027$) compared to the CON group (Figure 3B). At week 4, the SJZD group exhibited significantly higher levels of $CD3^+$ ($P < .001$) and $CD19^+$ ($P = .003$) compared to the CON group (Figure 3B).

Inflammatory-related indices. Inflammation-related cytokines were measured to assess the inflammation in postoperative NSCLC patients (Figure 3C). At week 1, the IL-8 level in the SJZD group (59.34 ± 65.62) was lower than CON group (118.11 ± 110.81) ($P = .004$). The IL-10 level was increased in the SJZD group (10.52 ± 23.56) and decreased in CON group (5.14 ± 0.35) ($P = .004$). Compared to baseline and week 1, after 4 weeks of treatment, both SJZD (52.37 ± 91.71) and CON group (52.49 ± 31.20) greatly downregulated IL-8 level ($P = .005$). In comparison to the baseline, the IL-10 level was increased in SJZD group (7.97 ± 4.50) and decreased in CON group (5.12 ± 0.30) ($P = .003$).

OTU Classification of Gut Microbiota

The study obtained a total of 6 095 582 high-quality readings from the 122 fecal samples. After quality and chimera checking, OTUs were determined based on a 97% similarity. The range of 16 S rRNA sequencing coverage was 400 to 440 bp (Supplemental Figure 1: quality sequence length distribution map).

Rank-abundance and rarefaction. The rank-abundance curves in both groups showed similar steepness and shortness at baseline, suggesting that the gut microflora had low relative abundance and evenness after surgery (Supplemental Figure 2A). During week 1 and week 4, the rank-abundance curves exhibited a consistent trend of becoming smoother and flatter, indicating a high level of species diversity and uniformity in the fecal samples (Supplemental Figure 2B-C). Moreover, the species curves exhibited a gradual increase in length in the SJZD group compared to the CON group, indicating that SJZD resulted in a greater enhancement of species abundances.

The rarefaction curves for each sample tended to approach the saturation plateau (Supplemental Figure 2D-F), showing a satisfactory sequencing depth and excellent coverage for all samples. At baseline, the rarefaction curves of SJZD and CON were similar (Supplemental Figure 2D). Between week 1 and week 4, significant changes were observed in the proportions of gut microbiota in 2 groups. Moreover, the OTU abundance of the SJZD group exhibited a gradual increase in comparison with the CON group (Supplemental Figure 2E-F).

Clustering analysis of OTU. The total number of OTUs generated in both groups decreased gradually from the baseline to week 4 (Figure 4). Nevertheless, the disparities between 2 groups escalated, with the SJZD group having a greater number of OTUs compared to the CON group (Baseline: 766 vs 772; Week 1: 697 vs 593; Week 4: 602 vs 402). Moreover, the SJZD group experienced a rise in the count of distinct OTUs, whereas the CON group experienced a decline in the count of distinct OTUs. As time passed, the disparities between the 2 groups became more apparent (Baseline: 194 vs 200; Week 1: 278 vs 174; Week 4: 270 vs 70).

Diversity of Gut Microbiota Within and Between Communities

Alpha diversity (α-diversity). The analysis of the species diversity of gut microbiota (Figure 5A-D) is crucial for the formation of distinct microbial communities, as it determines the species composition and distribution. At week 1, in the SJZD group, there were increases in the Chao, Shannon, and Sobs indices, along with a decline in the Simpson index. Conversely, the CON group exhibited completely opposite outcomes ($P > .05$). Following a 4-week treatment period, the SJZD group exhibited a notably greater Sobs index compared to the CON group ($P = .030$) (Figure 5B).

Beta diversity (β-diversity). In the first week, the PCoA analysis revealed a slight variation in the species diversity and community structure of gut microbiota between the 2 groups (PC1 = 16.19%, PC2 = 8.73%, $P = .075$) as shown in Figure 5F. The Beta diversity of the SJZD and CON group showed significant differences at week 4, with PC1 = 19.73% and PC2 = 10.92% as the x and y coordinates (ANOSIM R = .0617, $P = .016$) (Figure 5G). The points within each cluster collected distinctly, whereas the points separating the 2 clusters were relatively distant from one another on the coordinate graph, with the disparity being most noticeable at week 4 (Figure 5E-G).

In general, the analysis of microbial diversity revealed that in postoperative NSCLC patients, SJZD enhanced the abundance, diversity, and regulated the structure of the gut microbial community.

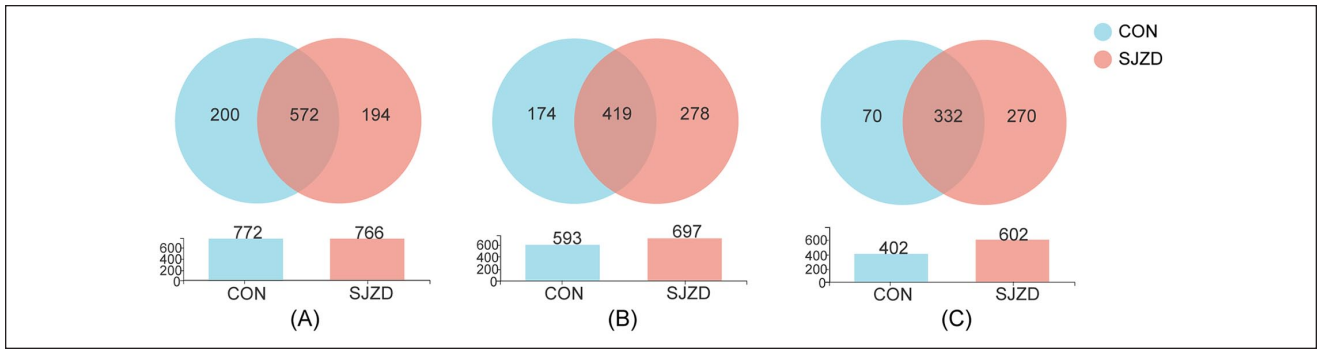

Figure 4. Venn diagrams of OTU clustering analysis in the SJZD and CON: (A) OTU Venn diagram at baseline, (B) OTU Venn diagram at week 1, and (C) OTU Venn diagram at week 4.

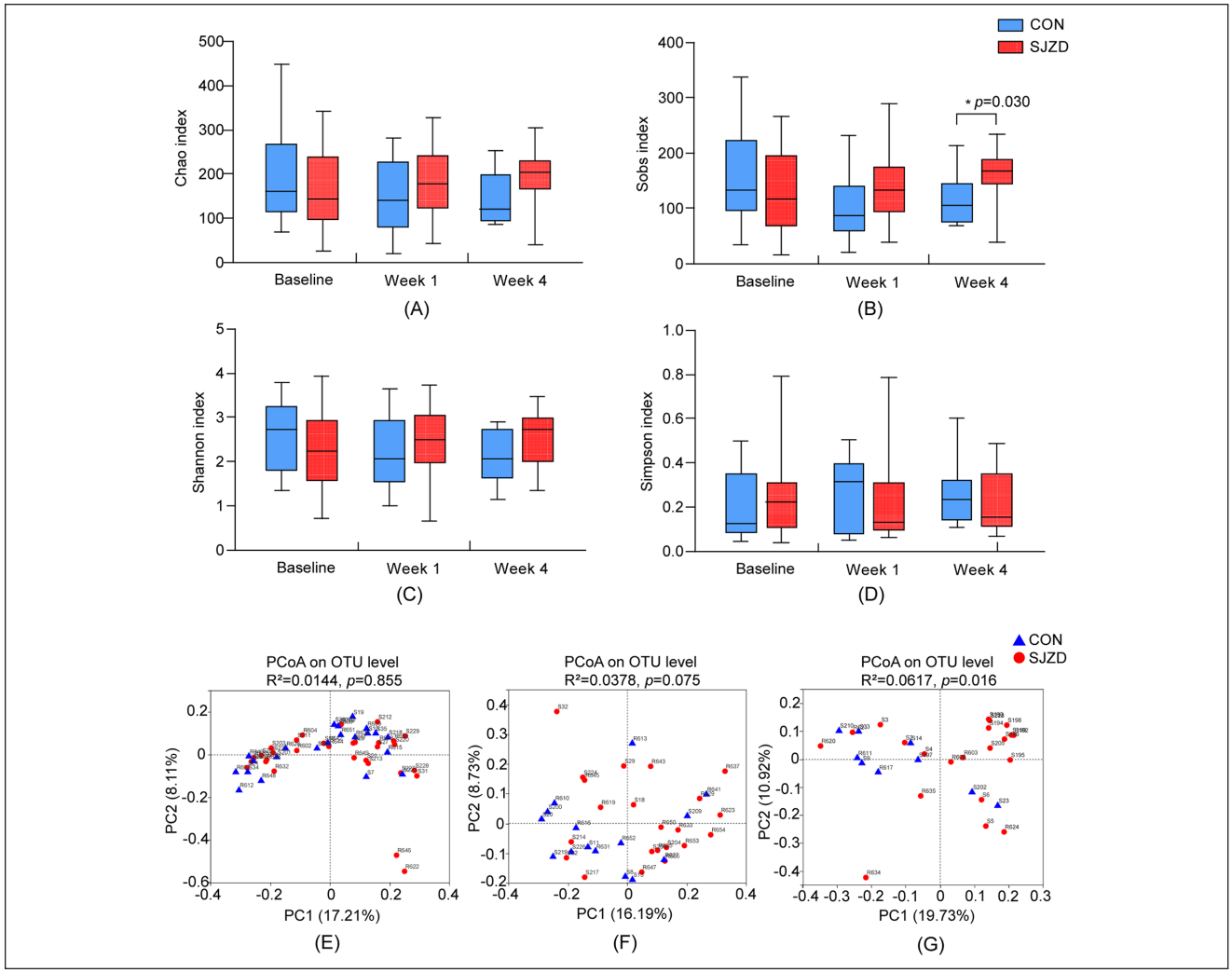

Figure 5. Alpha diversity and Beta diversity of gut microbiota in the SJZD and CON: (A) Chao index of Alpha diversity, (B) Sobs index of Alpha diversity, (C) Shannon index of Alpha diversity, (D) Simpson index of Alpha diversity, (E) Beta diversity at baseline, (F) Beta diversity at week 1, and (G) Beta diversity at week 4. *$P < .05$. The Chao, Shannon, Sobs indices are positively correlated with richness and diversity, while the Simpson index is negatively associated with species diversity. The more similar the community structure of the samples is, the closer they are to each other in the PCoA coordinate diagram. Samples with high similarity in community structure tended to cluster together, while those with very different communities were far apart.

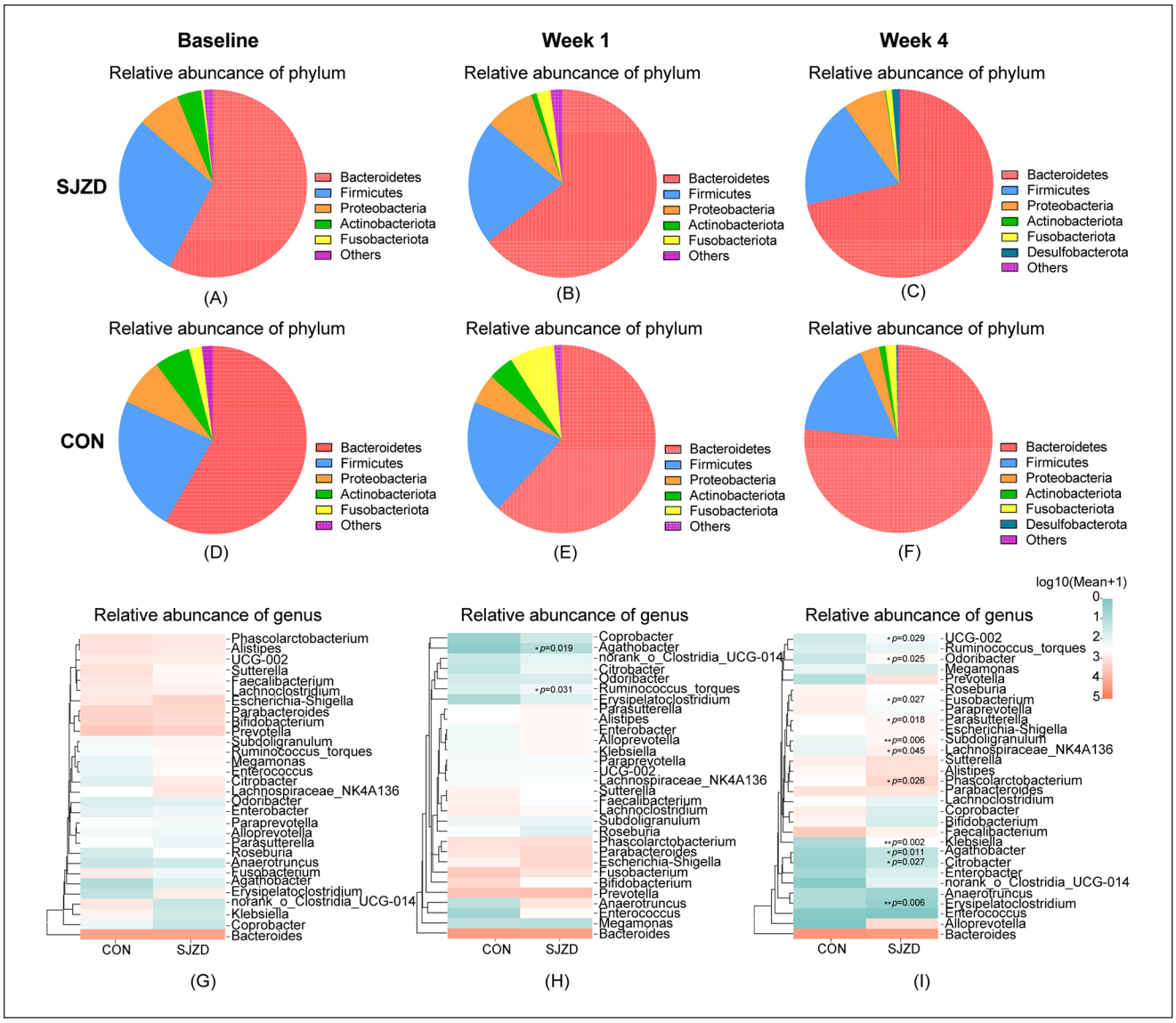

Figure 6. Major OTUs on phylum and genus level of gut microbiota in the SJZD and CON: (A) relative abundance of phylum level in the SJZD group at baseline, (B) relative abundance of phylum level in the SJZD group at week 1, (C) relative abundance of phylum level in the SJZD group at week 4, (D) relative abundance of phylum level in the CON group at baseline, (E) relative abundance of phylum level in the CON group at week 1, (F) relative abundance of phylum level in the CON group at week 4, (G) genus classification heatmap at baseline, (H) genus classification heatmap at week 1, and (I) genus classification heatmap at week 4. The color gradient of the heatmaps represents the mean abundance. The color gradient from green to red indicates that the mean abundances between the SJZD and the CON group are from low to high. $^{*}P < .05$.$^{**}P < .01$.

Taxonomic Profiling of Gut Microbiota

Taxonomic composition profiling at phylum and genus levels. At the phylum level, the most prevalent gut microbiota identified were Bacteroidetes, Firmicutes, Proteobacteria, Actinobacteriota, and Fusobacteriota in both groups at baseline, and after 1 week, as indicated by their abundance (Figure 6A, B, D, and E). In the SJZD and CON group, at week 4, the dominant microbial phyla were Bacteroidetes, Firmicutes, Proteobacteria, Actinobacteriota, Fusobacteriota, and Desulfobacterota, collectively representing more than 99% of the gut microbiota (Figure 6C and F). By week 4, there was a significant difference in the prevalence of Desulfobacterota and Fusobacteriota between the SJZD and CON group. In particular, Desulfobacterota ($P = .028$) showed a noticeably higher abundance in the SJZD group, while the CON group displayed a higher richness of Fusobacteriota ($P = .027$).

An analysis of the microbial composition focusing on the genus level was conducted to investigate gut microbial composition of SJZD (Figure 6G-I). The SJZD group displayed a notably greater abundance of Agathobacter ($P = .019$) and Ruminococcus_torques_group ($P = .031$) compared to the CON group at week 1. This difference in genus abundance was more statistically significant by the fourth week (Figure 6I). There were notable variations in 11 genera between the SJZD and the CON group. In particular, the levels of Citrobacter ($P = .027$), Klebsiella ($P = .002$), Lachnospiraceae_NK4A136_group ($P = .045$), Phascolarctobacterium ($P = .026$), UCG002_f_Oscillospiraceae ($P = .029$), Agathobacter ($P = .011$), Parasutterella ($P = .018$), Odoribacter ($P = .025$), and Subdoligranulum ($P = .006$) exhibited a higher presence in the SJZD group when compared to the CON group. In the SJZD group, the levels of Erysipelatoclostridium ($P = .006$) and Fusobacterium ($P = .027$) were significantly reduced. By enhancing the presence of probiotic microorganisms and reducing the presence of harmful bacteria, SJZD exhibited the potential to modify the gut microbial composition and structure.

Gut microbial biomarkers in postoperative NSCLC patients by LEfSe analysis. At baseline, LEfSe completely detected 12 microorganisms exhibiting significant differences, with 3 and 9 microorganisms respectively found in the SJZD and CON groups (Figure 7A and B).

At week 1, notable variations were observed in the SJZD and CON groups, with 9 and 2 distinct microorganisms identified, respectively (Figure 7C and D). Dominant species in the SJZD group included g__Enterobacter, g__Agathobacter, g__Ruminococcus_torques_group, f__Erysipelatoclostridiaceae, o__Eubacteriales, f__Eubacteriaceae, g__Eubacterium, g__Eubacterium_siraeum_group, f__Anaerovoracaceae. The CON group was characterized by the prominent presence of g__Lachnospiraceae_UCG-010 and c__Alphaproteobacteria. At week 4, totally, 34 and 14 microbes with significant differences were enriched in the SJZD and CON group respectively (Figure 7E and F). While both groups experienced noticeable increases in the number of gut microbial biomarkers, the SJZD group exhibited a greater abundance of these biomarkers. The gut microbiota in the SJZD group exhibited significantly higher levels of o__Acidaminococcales, f__Acidaminococcaceae, g__Phascolarctobacterium, g__Parasutterella, f__Marinifilaceae, g__Odoribacter, g__Lachnospiraceae_NK4A136_group, g__Subdoligranulum, p__Desulfobacterota, f__Desulfovibrionaceae, g__Ruminococcus, g__Desulfovibrio, g__Agathobacter, g__Coprococcus, g__Christensenellaceae_R-7_group, f__Christensenellaceae, and g__Butyricimonas. The CON group significantly had higher levels of g__Flavonifractor, f__Anaerolineaceae, o__Anaerolineales,c__Anaerolineae,p__Chloroflexi,g__Intestinibacter, g__Eggerthella, g__unclassified_o__Burkholderiales,g__Hungatella,g__Erysipelatoclostridium, and g__Sellimonas. Collectively, these findings demonstrated that the SJZD group and the CON group had significantly different predominant microbial biomarkers after SJZD treatment, with the SJZD group exhibiting significantly more probiotic microbes and less pathogenic microbes.

Co-occurrence Network Analysis in Gut Microbiota

From week 1 to week 4, there was a gradual increase in the modularity values and the number of modules in both the SJZD group and CON group (Figure 8). The SJZD group exhibited superior community partitioning compared to the CON group, evident by its higher level of modularity value and number of modules. The results of the co-occurrence network analysis revealed that the SJZD group had better co-occurrence interactions and possessed more characteristics of community partitioning. The analysis of co-occurring networks demonstrated the ecological relationships among OTUs at the genus level, suggesting that SJZD treatment had modified the microbial structure. Several topological indices were also calculated to assess the characteristics of the co-occurrence networks (Supplemental Table 1).

Gut Microbiome Functional Prediction

There was no notable disparity in the KEGG pathways between the 2 groups at the start and after 1 week (Figure 9A). In the fourth week, significant variances were observed in the 12 biological pathways associated with the functional prediction of gut microbiota within the Level 3 classification of KEGG pathways between 2 groups (Figure 9B). More specifically, the SJZD group exhibited a notable rise in the 3 metabolic pathways. The pathways included nonribosomal peptide structures (ko01054) ($P = .005$), flavonoid biosynthesis (ko00941) ($P = .021$), stilbenoid, diarylheptanoid and gingerol biosynthesis (ko00945) ($P = .021$). Additionally, there was an upregulation in 1 cellular processes pathway, namely meiosis-yeast (ko04113) ($P = .011$), and 1 organismal systems pathway, which was mineral absorption (ko04978) ($P = .024$).

In the meantime, the SJZD group significantly downregulated the activities of 4 organismal system pathways associated with bile secretion (ko04976) ($P = .010$), retrograde endocannabinoid signaling (ko04723) ($P = .014$), parathyroid hormone synthesis, secretion and action (ko04928) ($P = .025$), and GnRH signaling pathway (ko04912) ($P = .025$). Additionally, SJZD downregulated 2

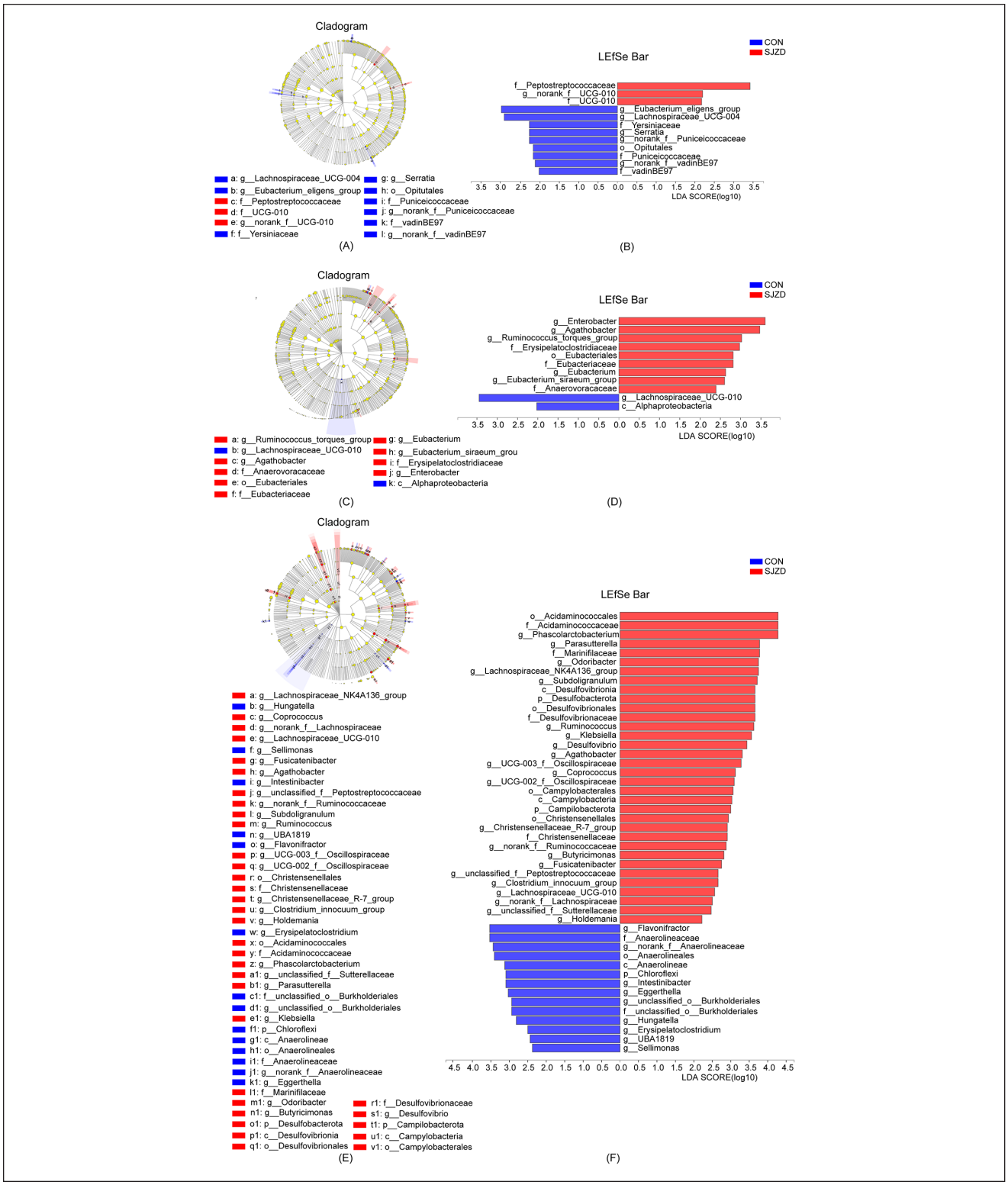

Figure 7. Gut microbial biomarkers identified by LEfSe analysis in the SJZD and CON. The dominant gut microbial biomarkers were displayed by the histogram of LDA value distribution and cladogram. (A) LEfSe analysis cladogram at baseline. (B) LEfSe analysis histogram of LDA value distribution at baseline. (C) LEfSe analysis cladogram at week 1. (D) LEfSe analysis histogram of LDA value distribution at week 1. (E) LEfSe analysis cladogram at week 4. (F) LEfSe analysis histogram of LDA value distribution at week 4. The logarithmic LDA score > 2.0 and $P < .05$ are regarded as the gut microbial biomarkers with significantly statistical difference.

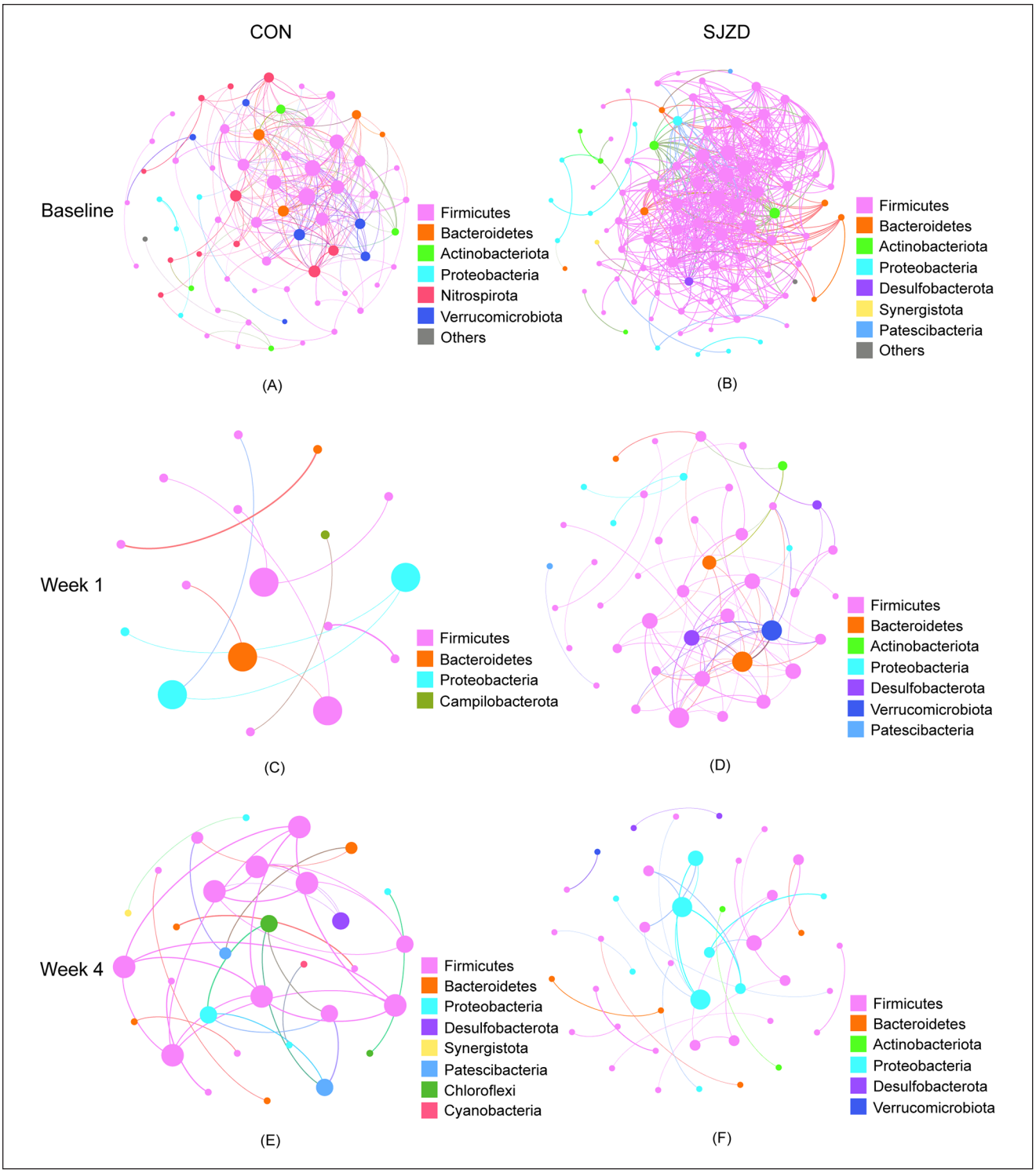

Figure 8. Co-occurrence network analysis of gut microbiota in the SJZD and CON. The co-occurrence networks of (A) CON group at baseline, (B) SJZD group at baseline, (C) CON group at week 1, (D) SJZD group at week 1, (E) CON group at week 4, and (F) SJZD group at week 4. The nodes in the figure represent OTUs at the genus level, and the edges (the line between 2 nodes) represent the significant positive correlation between 2 OTUs (Spearman $|\rho| \geq .6$, adjust $P < .01$). The node size is scaled according to their degree of interaction. The thickness of the edges corresponds to the size of the correlations. The different colors represent the different modules by modularity clustering, and the node label is the OTU classification at genus level in the networks.

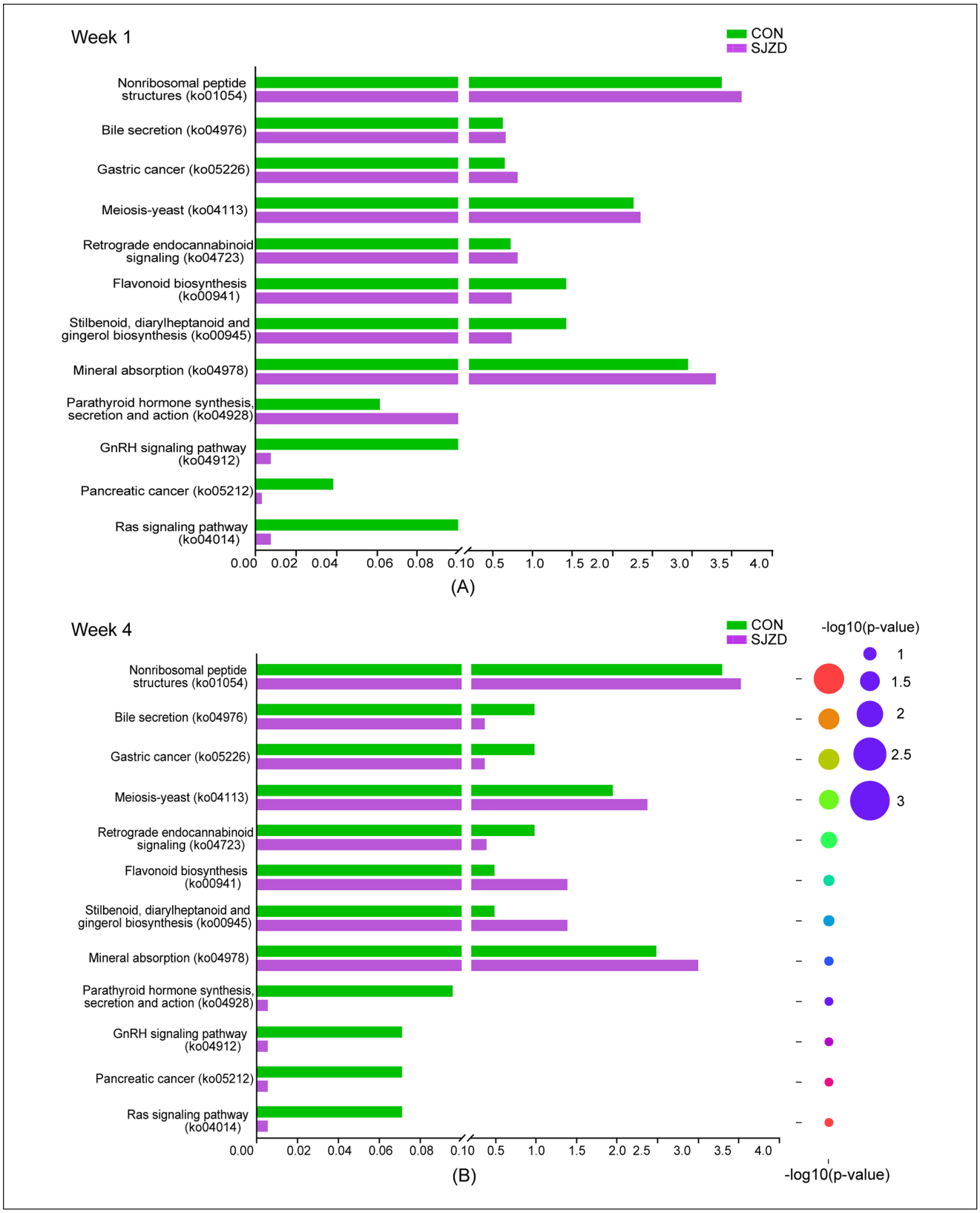

Figure 9. Gut microbiome functional prediction of KEGG level 3 pathway in the SJZD and CON. (A) The relative abundance of KEGG level 3 pathway differentially enriched in the SJZD and CON group at week 1. (B) The relative abundance of KEGG level 3 pathway differentially enriched in the SJZD and CON group at week 4.

pathways related to human diseases, which were gastric cancer (ko05226) ($P = .010$) and pancreatic cancer (ko05212) ($P = .025$). Furthermore, SJZD negatively impacted 1 environmental information processing pathway, specifically the Ras signaling pathway (ko04014) ($P = .025$). Overall, these findings suggested that SJZD has the ability to regulate the functional pathways and improve the dysfunctions of the gut microbiota in postoperative NSCLC.

Discussion

Surgical intervention is the preferred therapeutic approach for early-stage lung cancer. Nevertheless, patients may experience long-term diminished QOL, gastrointestinal dysfunction, and abnormal serum indices following the procedure.[44] Consequently, the rehabilitation of NSCLC patients after surgery continues to present challenges.[45] To the best of our understanding, this is the first prospective observational study investigating the effects of SJZD on QOL, immune functions, inflammation, and gut microbiota in postoperative NSCLC patients up till now.

This observational study demonstrated that the administration of SJZD had a beneficial effect on the QOL, physiological functioning, discomfort reduction, immune response regulation, and inflammation suppression in postoperative NSCLC patients. Notably, within a 4-week post-surgery period, a discernible deterioration in both physical and cognitive functioning was observed, indicating the substantial impact of surgical interventions on individuals with early-stage NSCLC, primarily resulting in physical and cognitive impairment. Importantly, the administration of SJZD significantly augmented both physical and cognitive capacities. According to these findings, SJZD demonstrated improvements in postoperative symptoms such as dyspnea, coughing, hemoptysis, and pain. Numerous studies have indicated that SJZD exhibits an anti-cancer efficacy as well as a synergistic effect in preventing cancer cachexia, alleviating inflammatory response, improving malnutrition state, and enhancing QOL.[23,24,46-48]

Surgical operations and interventions performed during the perioperative phase can impact immune surveillance and the inflammatory response.[49] The extraction of different monosaccharide compositions from SJZD has noticeable effects on intestinal immunity, specific immunity, and nonspecific immunity.[50] It has the capability to augment the adaptive immune response, regulate the intestinal immune system, and facilitate the restoration of gastrointestinal function, which is through the reduction of $CD3^+$T cells and $CD8^+$T cells, and the elevation of $CD4^+$T cells.[51] Furthermore, SJZD has demonstrated efficacy in mitigating inflammation by enhancing intestinal local immunity.[52] In this study, it was observed that SJZD exerted a notably positive impact on immune cells, specifically $CD3^+$, $CD3^+CD4^+$, and $CD3^+CD8^+$, while concurrently elevating the levels of the anti-inflammatory cytokine IL-10 and significantly diminishing the levels of the proinflammatory cytokine IL-8. In summary, SJZD played a pivotal role in regulating the level of immune cells and inflammatory cells in postoperative NSCLC patients.

The disruption of the gut-lung axis has the potential to lead to the colonization of pathogens, translocation of bacteria, oxidative stress, impairment of intestinal barrier, exposure to toxins, metabolic disturbance, persistent inflammation, and immune dysregulation.[53] Microbial dysbiosis is a prevalent occurrence in lung cancer patients, as evidenced by reduced species diversity, alterations in microbial composition, instability in structural integrity, and impaired biological functions.[54-56] This study indicated the presence of dysbacteriosis in NSCLC patients who have recently undergone surgery. SJZD has been found to exert a significant influence on regulating the gut microbiota, contributing to increased microbial abundance and species diversity. Total polysaccharides of the SJZD alleviate the impairment of the intestinal epithelial cell barrier function.[57] Previous studies have consistently shown that SJZD enhanced the diversity and constitution of the gut microbiota, while also exerting an immunomodulatory influence by regulating the gut microbiota.[26,50,58]

Recent discoveries have highlighted a strong association between metabolites generated by the gut microbiome and human health.[59] Short-chain fatty acids (SCFAs) are the metabolic fermentation products of the gut microbiota. The presence and progression of various diseases, including multiple types of cancer, are strongly linked to the decrease in SCFAs and probiotics that produce SCFAs.[60] SCFAs have been proven to exert a regulatory influence on immune function, inflammation, and metabolism.[61] Butyrate is one of the main SCFAs produced by intestinal microorganisms. Reductions in colonic butyrate concentrations disrupt the integrity of the barrier and promote inflammation.[62] Furthermore, patients with NSCLC have been reported to exhibit dysbiosis in gut bacteria responsible for butyrate production.[63] The LEfSe analysis demonstrated a statistically significant increase in gut microbiota biomarkers by the fourth week in both groups. SJZD significantly increased the abundance of numerous probiotic microbiota, which in turn enhanced the production of SCFAs. Previous studies have identified Agathobacter,[64] Eubacterium,[65] Ruminococcus,[66] Subdoligranulum,[67] Phascolarctobacterium,[68] and Odoribacter as key symbiont microbiota in the gut ecosystem that contribute to SCFA generation.[69] These microbiota have been shown to exert a modulatory effect on antitumor immune responses, inflammation suppression, and cancer inhibition. A study has shown that Ruminococcus has a positive impact on the intestinal inflammation and the $CD8^+$/Forkhead box protein3 $(Foxp3)^+CD4^+$ ratio in the tumor microenvironment.[66] The presence of Subdoligranulum in humans is positively

associated with microbial diversity, but has a negative correlation with levels of C-reactive protein (CRP) and IL-6.[70] Odoribacter splanchnicus has been discovered to mitigate T cell inflammation and colitis by increasing the population of Foxp3$^+$/retinoic acid receptor-related orphan receptor γt (RORγt)$^+$ regulatory T (Treg) cells, stimulating IL-10 synthesis, and generating SCFAs.[71] The bacteria of Christensenellaceae and Eubacterium have been proposed as promising therapeutic agents, representing a new generation of probiotics.[72] The present study demonstrated that SJZD had a notable effect on enhancing the population of probiotic bacteria that produce SCFAs as mentioned above. Generally speaking, the findings of this study revealed that SJZD effectively alleviated the disturbance of the symbiotic microbiome and reestablished a new intestinal microecology equilibrium of postoperative NSCLC through the promotion of abundance and diversity of gut microbiota, and the augmentation of probiotic microbes capable of producing SCFAs.

Extensive studies have revealed significant variations in microbiome functions between individuals with NSCLC and those in a healthy state, with particular emphasis on the decline of metabolic pathways and alterations in metabolites.[56,73,74] The present study demonstrated that SJZD significantly upregulated metabolism pathways associated with nonribosomal peptide structures, flavonoid biosynthesis, stilbenoid, and diarylheptanoid biosynthesis. These compounds have demonstrated promising effects against tumors, along with possessing antioxidant, anti-inflammatory, and immune-enhancing properties in various cancer types.[75-78] Bidirectional interactions have been observed between gut microbiota and flavonoid, stilbenoid, and diarylheptanoid compounds, and these interactions manifest through direct and indirect mechanisms, encompassing gut microbiota modulation, T cell differentiation regulation, intestinal barrier function enhancement, inflammatory pathway regulation, and reduction of oxidative stress.[79-81] Bile acids, as metabolites of the intestinal microbiota, have been shown to modulate antitumor immunity and regulate immunological homeostasis.[82] The metabolites of bile acids directly control the equilibrium of T helper cell 17 (Th17) and Treg cells, thus impacting the immune responses of the host.[83,84] SJZD significantly downregulated the bile secretion pathway in this study, which is known to be increased in NSCLC patients compared to healthy individuals according to a previous study.[56] In conclusion, the findings suggested that SJZD played a role in restoring a healthy functional state of the gut microbiota in postoperative NSCLC.

However, there are still several limitations in this study. Due to the absence of the random design, some biases are difficult to avoid. The study of the gut microbiome is inherently complex, as it is influenced by numerous confounding factors such as geographical environment, lifestyle, dietary habits, psychological stress, physiological characteristics, and other individual differences and interferences.[85] Achieving complete elimination of bias in this field is challenging. Therefore, it is imperative to recruit a larger number of patients from multiple centers, collect a greater quantity of clinical data and fecal samples, and extend the duration of observation in order to enhance the validation of the association between the impact of SJZD on the regulation of gut microbiota. Furthermore, the therapeutic effects of SJZD involve intricate mechanisms, multiple targets and signaling pathways, thus necessitating further study to explore the underlying mechanisms implicated.

Conclusions

The study demonstrated that SJZD exhibited the potential to improve QOL, reinstate immune equilibrium, alleviate inflammation, and regulate gut microbiota imbalance in postoperative NSCLC patients. SJZD may serve as a promising therapeutic intervention for complementary treatment of postoperative NSCLC, and requires more clinical research.

List of Abbreviation

ANOSIM	Analysis of similarities
AJCC	American Joint Committee on Cancer
ALT	Alanine aminotransferase
AST	Aspartate aminotransferase
CI	Confidence interval
CON	Control group
CRP	C-reaction protein
DNA	Deoxyribo nucleic acid
ELISA	Enzyme-linked immunosorbent assay
EORTC	European Organization for Research and Treatment of Cancer
ERAS	Enhanced recovery after surgery
FCM	Flow cytometry (FCM)
FOXP3	Forkhead box protein 3
GHS	Global health status
GMP	Good manufacturing practice
IQR	Interquartile range
IL	Interleukin
KEGG	Kyoto Encyclopedia of Genes and Genomes
KPS	Karnofsky Performance Status
KW	Kruskal-Wallis
LS	Least-squares
LEfSe	Linear discriminant analysis effect size
LDA	Linear discriminant analysis
NSCLC	Non-small-cell lung cancer
OTU	Operational Taxonomic Unit
PCR	Polymerase chain reaction
PCoA	Principal coordinate analysis
PD	Phylogenetic diversity

PICRUSt2	Phylogenetic Investigation of Communities by Reconstruction of Unobserved States 2
QOL	Quality of life
QLQ-C30	Quality of Life Questionnaire Core 30
QLQ-LC13	Quality of Life Questionnaire Lung Cancer Module 13
RDP	Ribosomal Database Project
RNA	Ribonucleic Acid
ROR γt	Retinoic acid receptor-related orphan receptor γt
SEM	Standard error of mean
SCFA	Short-chain fatty acid
SJZD	Si-Jun-Zi decoction
TNF-α	Tumor necrosis factor-alpha
TCM	Traditional Chinese Medicine.
Th17	T helper cell 17
Treg	Regulatory T cell.

Acknowledgments

We would like to thank all the patients for participating in this study, completing the data collection, and providing the fecal samples.

Author Contributions

Yiyun He: Conceptualization, Data curation, Formal analysis, Investigation, Validation, Writing - original draft. Ao Qi: Investigation. Yifeng Gu: Investigation. Congmeng Zhang: Investigation. Yichao Wang: Investigation. Wenxiao Yang, Project administration. Ling Bi, Data curation, Project administration. Yabin Gong: Project administration, Resources. Lijing Jiao: Conceptualization, Project administration, Resources, Supervision, Writing—review & editing. Ling Xu: Conceptualization, Project administration, Resources, Supervision, Writing—review & editing. All authors read and approved the final manuscript. Lijing Jiao and Ling Xu both are equal corresponding author and have overall responsibility.

Availability of Data and Material

All datasets generated and analyzed during the current study are available from the corresponding author on reasonable request. The original 16S rRNA sequencing raw data were deposited into the online repositories NCBI database (Accession Number: PRJNA982600).

Declaration of Conflicting Interests

The author(s) declared no potential conflicts of interest with respect to the research, authorship, and/or publication of this article.

Funding

The author(s) disclosed receipt of the following financial support for the research, authorship, and/or publication of this article: This work was supported by the National Natural Science Foundation of China (grant number 82074339); the Shanghai Natural Science Foundation (grant number 22ZR1462400, 20ZR1459400); the Medical Innovation Research Project of Science and Technology Innovation Plan of Shanghai Science and Technology Commission (grant number 22Y31920400); and the Clinical Cooperation pilot project of traditional Chinese and Western medicine of Shanghai Municipal Health Commission (grant number ZXYXZ-201901).

Ethics Approval and Consent to Participate

This study was approved by the Ethics Committee of Yueyang Hospital of Integrated Traditional Chinese and Western Medicine affiliated with Shanghai University of Traditional Chinese Medicine (No.2020-038). This study was conducted according to the World Medical Association declaration of Helsinki. Written informed consents were obtained from all the participants before taking part in this study. The privacy rights of human subjects were always observed.

ORCID iD

Yiyun He https://orcid.org/0000-0002-3090-7063

Supplemental Material

Supplemental material for this article is available online.

References

1. Siegel RL, Miller KD, Wagle NS, Jemal A. Cancer statistics, 2023. *CA Cancer J Clin*. 2023;73:17-48. doi:10.3322/caac.21763
2. Bendixen M, Jørgensen OD, Kronborg C, Andersen C, Licht PB. Postoperative pain and quality of life after lobectomy via video-assisted thoracoscopic surgery or anterolateral thoracotomy for early stage lung cancer: a randomised controlled trial. *Lancet Oncol*. 2016;17:836-844. doi:10.1016/S1470-2045(16)00173-X
3. Ding Q, Chen W, Gu Y, et al. Accelerated rehabilitation combined with enteral nutrition in the management of lung cancer surgery patients. *Asia Pac J Clin Nutr*. 2020;29:274-279. doi:10.6133/apjcn.202007_29(2).0010
4. Furák J, Németh T, Lantos J, et al. Perioperative systemic inflammation in lung cancer surgery. *Front Surg*. 2022;9:883322. doi:10.3389/fsurg.2022.883322
5. An N, Dong W, Pang G, Zhang Y, Liu C. TPVB and general anesthesia affects postoperative functional recovery in elderly patients with thoracoscopic pulmonary resections based on ERAS pathway. *Transl Neurosci*. 2023;14:20220305. doi:10.1515/tnsci-2022-0305
6. Rogers LJ, Bleetman D, Messenger DE, et al. The impact of enhanced recovery after surgery (ERAS) protocol compliance on morbidity from resection for primary lung cancer. *J Thorac Cardiovasc Surg*. 2018;155:1843-1852. doi:10.1016/j.jtcvs.2017.10.151
7. Forster C, Doucet V, Perentes JY, et al. Impact of an enhanced recovery after surgery pathway on thoracoscopic lobectomy outcomes in non-small cell lung cancer patients: a propensity score-matched study. *Transl Lung Cancer Res*. 2021;10:93-103. doi:10.21037/tlcr-20-891
8. Licker M, Hagerman A, Bedat B, et al. Restricted, optimized or liberal fluid strategy in thoracic surgery: A narrative

review. *Saudi J Anaesth*. 2021;15:324-334. doi:10.4103/sja.sja_1155_20
9. Wang J, Zhang W, Wang M, et al. Perioperative alterations in the intestinal microbiota and functional changes mediate innate immune activation after small bowel transplantation. *Life Sci*. 2021;277:119468. doi:10.1016/j.lfs.2021.119468
10. Lukovic E, Moitra VK, Freedberg DE. The microbiome: implications for perioperative and critical care. *Curr Opin Anaesthesiol*. 2019;32:412-420. doi:10.1097/ACO.0000000000000734
11. Wang GY, Chen SY, Chen YY, et al. Protective effect of rosmarinic acid-rich trichodesma khasianum clarke leaves against ethanol-induced gastric mucosal injury in vitro and in vivo. *Phytomedicine*. 2021;80:153382. doi:10.1016/j.phymed.2020.153382
12. Liao L, Schneider KM, Galvez EJC, et al. Intestinal dysbiosis augments liver disease progression via NLRP3 in a murine model of primary sclerosing cholangitis. *Gut*. 2019;68:1477-1492. doi:10.1136/gutjnl-2018-316670
13. Yu ZW, Xie Y, Huang ZC, et al. Study of the therapeutic effect of raw and processed Vladimiriae Radix on ulcerative colitis based on intestinal flora, metabolomics and tissue distribution analysis. *Phytomedicine*. 2021;85:153538. doi:10.1016/j.phymed.2021.153538
14. Ge Y, Wang X, Guo Y, et al. Gut microbiota influence tumor development and alter interactions with the human immune system. *J Exp Clin Cancer Res*. 2021;40:42. doi:10.1186/s13046-021-01845-6
15. Zhao Y, Liu Y, Li S, et al. Role of lung and gut microbiota on lung cancer pathogenesis. *J Cancer Res Clin Oncol*. 2021;147:2177-2186. doi:10.1007/s00432-021-03644-0
16. Dong B, Peng C, Ma P, Li X. An integrated strategy of MS-network-based offline 2DLC-QTOF-MS/MS coupled with UHPLC-QTRAP(®)-MS/MS for the characterization and quantification of the non-polysaccharides in Sijunzi decoction. *Anal Bioanal Chem*. 2021;413:3511-3527. doi:10.1007/s00216-021-03302-x
17. Wang Y, He S, Cheng X, et al. UPLC-Q-TOF-MS/MS fingerprinting of Traditional Chinese Formula SiJunZiTang. *J Pharm Biomed Anal*. 2013;80:24-33. doi:10.1016/j.jpba.2013.02.021
18. Guan Z, Wang M, Cai Y, et al. Rapid characterization of the chemical constituents of Sijunzi decoction by UHPLC coupled with Fourier transform ion cyclotron resonance mass spectrometry. *J Chromatogr B Analyt Technol Biomed Life Sci*. 2018;1086:11-22. doi:10.1016/j.jchromb.2018.04.009
19. Dong B, Ma P, Chen X, et al. Drug-polysaccharide/herb interactions and compatibility rationality of Sijunzi decoction based on comprehensive pharmacokinetic screening for multi-components in rats with spleen deficiency syndrome. *J Ethnopharmacol*. 2023;302:115871. doi:10.1016/j.jep.2022.115871
20. Zhou JY, Chen M, Wu CE, et al. The modified Si-Jun-Zi decoction attenuates colon cancer liver metastasis by increasing macrophage cells. *BMC Complement Altern Med*. 2019;19:86. doi:10.1186/s12906-019-2498-4
21. Li C, Niu M, Wang R, et al. The modulatory properties of Si Jun Zi Tang enhancing anticancer of gefitinib by an integrating approach. *Biomed Pharmacother*. 2019;111:1132-1140. doi:10.1016/j.biopha.2018.12.026
22. Dai L, Zhou WJ, Wang M, Zhou SG, Ji G. Efficacy and safety of Sijunzi decoction for chronic fatigue syndrome with spleen deficiency pattern: study protocol for a randomized, double-blind, placebo-controlled trial. *Ann Transl Med*. 2019;7:587. doi:10.21037/atm.2019.09.136
23. Wang Z, Li T, Li R, et al. Sijunzi Tang improves gefitinib resistance by regulating glutamine metabolism. *Biomed Pharmacother*. 2023;167:115438. doi:10.1016/j.biopha.2023.115438
24. Li Y, Chen Y, Zeng Y, et al. Enteral nutrition combined with improved-Sijunzi decoction shows positive effect in Precachexia cancer patients: a retrospective analysis. *Evid Based Complement Alternat Med*. 2021;2021: 7357521. doi:10.1155/2021/7357521
25. Shi Y, Zhu H, Li R, et al. Effect of polysaccharides from Sijunzi decoction on Ca(2+) related regulators during intestinal mucosal restitution. *Phytomedicine*. 2019;58:152880. doi:10.1016/j.phymed.2019.152880
26. Ma P, Peng Y, Zhao L, Liu F, Li X. Differential effect of polysaccharide and nonpolysaccharide components in Sijunzi decoction on spleen deficiency syndrome and their mechanisms. *Phytomedicine*. 2021;93:153790. doi:10.1016/j.phymed.2021.153790
27. Qu L, Tan W, Yang J, et al. Combination compositions composed of l-glutamine and Si-Jun-Zi-Tang might be a preferable choice for 5-fluorouracil-induced intestinal mucositis: an exploration in a mouse model. *Front Pharmacol*. 2020;11:918. doi:10.3389/fphar.2020.00918
28. Aaronson NK, Ahmedzai S, Bergman B, et al. The European Organization for Research and Treatment of Cancer QLQ-C30: a quality-of-life instrument for use in international clinical trials in oncology. *J Natl Cancer Inst*. 1993;85:365-376. doi:10.1093/jnci/85.5.365
29. Bergman B, Aaronson NK, Ahmedzai S, Kaasa S, Sullivan M. The EORTC QLQ-LC13: a modular supplement to the EORTC Core Quality of Life Questionnaire (QLQ-C30) for use in lung cancer clinical trials. *Eur J Cancer*. 1994;30:635-642. doi:10.1016/0959-8049(94)90535-5
30. Han M, Hao L, Lin Y, et al. A novel affordable reagent for room temperature storage and transport of fecal samples for metagenomic analyses. *Microbiome*. 2018;6:43. doi:10.1186/s40168-018-0429-0
31. Su W, Du Y, Lian F, et al. Standards for collection, preservation, and transportation of fecal samples in TCM clinical trials. *Front Cell Infect Microbiol*. 2022;12:783682. doi:10.3389/fcimb.2022.783682
32. Casals-Pascual C, González A, Vázquez-Baeza Y, et al. Microbial diversity in clinical microbiome studies: sample size and statistical power considerations. *Gastroenterology*. 2020;158:1524-1528. doi:10.1053/j.gastro.2019.11.305
33. Ponziani FR, Putignani L, Paroni Sterbini F, et al. Influence of hepatitis C virus eradication with direct-acting antivirals on the gut microbiota in patients with cirrhosis. *Aliment Pharmacol Ther*. 2018;48:1301-1311. doi:10.1111/apt.15004
34. Chen S, Zhou Y, Chen Y, Gu J. Fastp: an ultra-fast all-in-one FASTQ preprocessor. *Bioinformatics*. 2018;34:i884-i890. doi:10.1093/bioinformatics/bty560

35. Magoč T, Salzberg SL. FLASH: fast length adjustment of short reads to improve genome assemblies. *Bioinformatics*. 2011;27:2957-2963. doi:10.1093/bioinformatics/btr507
36. Wang Q, Garrity GM, Tiedje JM, Cole JR. Naive Bayesian classifier for rapid assignment of rRNA sequences into the new bacterial taxonomy. *Appl Environ Microbiol*. 2007;73:5261-5267. doi:10.1128/aem.00062-07
37. Caporaso JG, Kuczynski J, Stombaugh J, et al. QIIME allows analysis of high-throughput community sequencing data. *Nat Methods*. 2010;7:335-336. doi:10.1038/nmeth.f.303
38. Crespo-Salgado J, Vehaskari VM, Stewart T, et al. Intestinal microbiota in pediatric patients with end stage renal disease: a Midwest Pediatric Nephrology Consortium study. *Microbiome*. 2016;4:50. doi:10.1186/s40168-016-0195-9
39. Lozupone C, Knight R. UniFrac: a new phylogenetic method for comparing microbial communities. *Appl Environ Microbiol*. 2005;71:8228-8235. doi:10.1128/aem.71.12.8228-8235.2005
40. Segata N, Izard J, Waldron L, et al. Metagenomic biomarker discovery and explanation. *Genome Biol*. 2011;12:R60. doi:10.1186/gb-2011-12-6-r60
41. Douglas GM, Maffei VJ, Zaneveld JR, et al. PICRUSt2 for prediction of metagenome functions. *Nat Biotechnol*. 2020;38:685-688. doi:10.1038/s41587-020-0548-6
42. Kanehisa M, Araki M, Goto S, et al. KEGG for linking genomes to life and the environment. *Nucleic Acids Res*. 2008;36:D480-D484. doi:10.1093/nar/gkm882
43. Langille MG, Zaneveld J, Caporaso JG, et al. Predictive functional profiling of microbial communities using 16S rRNA marker gene sequences. *Nat Biotechnol*. 2013;31:814-821. doi:10.1038/nbt.2676
44. Rauma V, Sintonen H, Räsänen JV, Salo JA, Ilonen IK. Long-term lung cancer survivors have permanently decreased quality of life after surgery. *Clin Lung Cancer*. 2015;16:40-45. doi:10.1016/j.cllc.2014.08.004
45. Lu Y, Yuan Z, Han Y, Zhang Y, Xu R. Summary of best evidence for enhanced recovery after surgery for patients undergoing lung cancer operations. *Asia Pac J Oncol Nurs*. 2022;9:100054. doi:10.1016/j.apjon.2022.03.006
46. Shang L, Wang Y, Li J, et al. Mechanism of Sijunzi decoction in the treatment of colorectal cancer based on network pharmacology and experimental validation. *J Ethnopharmacol*. 2023;302:115876. doi:10.1016/j.jep.2022.115876
47. Ding P, Guo Y, Wang C, et al. A network pharmacology approach for uncovering the antitumor effects and potential mechanisms of the Sijunzi decoction for the treatment of gastric cancer. *Evid Based Complement Alternat Med*. 2022;2022:9364313. doi:10.1155/2022/9364313
48. Zhou X, Li Y, Zhang M, et al. Spectrum-effect relationship between UPLC fingerprints and antilung cancer ffect of Si Jun Zi Tang. *Evid Based Complement Alternat Med*. 2019;2019:7282681. doi:10.1155/2019/7282681
49. Choi H, Hwang W. Perioperative inflammatory response and cancer recurrence in lung cancer surgery: a narrative review. *Front Surg*. 2022;9:888630. doi:10.3389/fsurg.2022.888630
50. Gao B, Peng Y, Peng C, Zhang Y, Li X. A cComparison of characterization and its actions on iImmunocompetent ells of polysaccharides from Sijunzi decoction. *Evid Based Complement Alternat Med*. 2019;2019:9860381. doi:10.1155/2019/9860381
51. Yu X, Cui Z, Zhou Z, et al. Si-jun-zi decoction treatment promotes the restoration of intestinal function after obstruction by regulating intestinal homeostasis. *Evid Based Complement Alternat Med*. 2014;2014:928579. doi:10.1155/2014/928579
52. Yu W, Lu B, Zhang H, Zhang Y, Yan J. Effects of the Sijunzi decoction on the immunological function in rats with dextran sulfate-induced ulcerative colitis. *Biomed Rep*. 2016;5:83-86. doi:10.3892/br.2016.678
53. Genua F, Raghunathan V, Jenab M, Gallagher WM, Hughes DJ. The role of gut barrier dysfunction and microbiome dysbiosis in colorectal cancer development. *Front Oncol*. 2021;11:626349. doi:10.3389/fonc.2021.626349
54. Zheng Y, Fang Z, Xue Y, et al. Specific gut microbiome signature predicts the early-stage lung cancer. *Gut Microbes*. 2020;11:1030-1042. doi:10.1080/19490976.2020.1737487
55. Zhao F, An R, Wang L, Shan J, Wang X. Specific gut microbiome and serum metabolome changes in lung cancer patients. *Front Cell Infect Microbiol*. 2021;11:725284. doi:10.3389/fcimb.2021.725284
56. Qin X, Bi L, Yang W, et al. Dysbiosis of the gut microbiome is associated with histopathology of lung cancer. *Front Microbiol*. 2022;13:918823. doi:10.3389/fmicb.2022.918823
57. Lu Y, Li L, Zhang JW, et al. Total polysaccharides of the Sijunzi decoction attenuate tumor necrosis factor-α-induced damage to the barrier function of a Caco-2 cell monolayer via the nuclear factor-κB-myosin light chain kinase-myosin light chain pathway. *World J Gastroenterol*. 2018;24:2867-2877. doi:10.3748/wjg.v24.i26.2867
58. Gao B, Wang R, Peng Y, Li X. Effects of a homogeneous polysaccharide from Sijunzi decoction on human intestinal microbes and short chain fatty acids in vitro. *J Ethnopharmacol*. 2018;224:465-473. doi:10.1016/j.jep.2018.06.006
59. Hezaveh K, Shinde RS, Klötgen A, et al. Tryptophan-derived microbial metabolites activate the aryl hydrocarbon receptor in tumor-associated macrophages to suppress anti-tumor immunity. *Immunity*. 2022;55:324-340.e8. doi:10.1016/j.immuni.2022.01.006
60. de Vos WM, Tilg H, Van Hul M, Cani PD. Gut microbiome and health: mechanistic insights. *Gut*. 2022;71:1020-1032. doi:10.1136/gutjnl-2021-326789
61. Goverse G, Molenaar R, Macia L, et al. Diet-derived short chain fatty acids stimulate intestinal epithelial cells to induce mucosal tolerogenic dendritic cells. *J Immunol*. 2017;198:2172-2181. doi:10.4049/jimmunol.1600165
62. Salvi PS, Cowles RA. Butyrate and the intestinal epithelium: modulation of proliferation and inflammation in homeostasis and disease. *Cells*. 2021;10:1775. doi:10.3390/cells10071775
63. Gui Q, Li H, Wang A, et al. The association between gut butyrate-producing bacteria and non-small-cell lung cancer. *J Clin Lab Anal*. 2020;34:e23318. doi:10.1002/jcla.23318
64. Martini G, Ciardiello D, Dallio M, et al. Gut microbiota correlates with antitumor activity in patients with mCRC and NSCLC treated with cetuximab plus avelumab. *Int J Cancer*. 2022;151:473-480. doi:10.1002/ijc.34033
65. Mukherjee A, Lordan C, Ross RP, Cotter PD. Gut microbes from the phylogenetically diverse genus Eubacterium and

their various contributions to gut health. *Gut Microbes*. 2020;12:1802866. doi:10.1080/19490976.2020.1802866
66. Messaoudene M, Pidgeon R, Richard C, et al. A natural polyphenol exerts antitumor activity and circumvents anti–PD-1 resistance through effects on the gut Microbiota. *Cancer Discov*. 2022;12:1070-1087. doi:10.1158/2159-8290.Cd-21-0808
67. Lloyd-Price J, Arze C, Ananthakrishnan AN, et al. Multi-omics of the gut microbial ecosystem in inflammatory bowel diseases. *Nature*. 2019;569:655-662. doi:10.1038/s41586-019-1237-9
68. Nagao-Kitamoto H, Leslie JL, Kitamoto S, et al. Interleukin-22-mediated host glycosylation prevents Clostridioides difficile infection by modulating the metabolic activity of the gut microbiota. *Nat Med*. 2020;26:608-617. doi:10.1038/s41591-020-0764-0
69. Sato Y, Atarashi K, Plichta DR, et al. Novel bile acid biosynthetic pathways are enriched in the microbiome of centenarians. *Nature*. 2021;599:458-464. doi:10.1038/s41586-021-03832-5
70. Van Hul M, Le Roy T, Prifti E, et al. From correlation to causality: the case of Subdoligranulum. *Gut Microbes*. 2020;12:1-13. doi:10.1080/19490976.2020.1849998
71. Lima SF, Gogokhia L, Viladomiu M, et al. Transferable immunoglobulin A-coated odoribacter splanchnicus in responders to fecal microbiota transplantation for ulcerative colitis limits colonic inflammation. *Gastroenterology*. 2022;162:166-178. doi:10.1053/j.gastro.2021.09.061
72. Singh TP, Natraj BH. Next-generation probiotics: a promising approach towards designing personalized medicine. *Crit Rev Microbiol*. 2021;47:479-498. doi:10.1080/1040841X.2021.1902940
73. Liu F, Li J, Guan Y, et al. Dysbiosis of the gut microbiome is associated with tumor biomarkers in lung cancer. *Int J Biol Sci*. 2019;15:2381-2392. doi:10.7150/ijbs.35980
74. Qian X, Zhang HY, Li QL, et al. Integrated microbiome, metabolome, and proteome analysis identifies a novel interplay among commensal bacteria, metabolites and candidate targets in non-small cell lung cancer. *Clin Transl Med*. 2022;12:e947. doi:10.1002/ctm2.947
75. Khan H, Ullah H, Martorell M, et al. Flavonoids nanoparticles in cancer: Treatment, prevention and clinical prospects. *Semin Cancer Biol*. 2021;69:200-211. doi:10.1016/j.semcancer.2019.07.023
76. Beetch M, Boycott C, Harandi-Zadeh S, et al. Pterostilbene leads to DNMT3B-mediated DNA methylation and silencing of OCT1-targeted oncogenes in breast cancer cells. *J Nutr Biochem*. 2021;98:108815. doi:10.1016/j.jnutbio.2021.108815
77. Guo CJ, Chang FY, Wyche TP, et al. Discovery of reactive microbiota-derived metabolites that inhibit host proteases. *Cell*. 2017;168:517-526.e18. doi:10.1016/j.cell.2016.12.021
78. Fan J, Wu M, Wang J, et al. 1,7-Bis(4-hydroxyphenyl)-1,4-heptadien-3-one induces lung cancer cell apoptosis via the PI3K/Akt and ERK1/2 pathways. *J Cell Physiol*. 2019;234:6336-6349. doi:10.1002/jcp.27364
79. Pei R, Liu X, Bolling B. Flavonoids and gut health. *Curr Opin Biotechnol*. 2020;61:153-159. doi:10.1016/j.copbio.2019.12.018
80. Wang M, Yu F, Zhang Y, Chang W, Zhou M. The effects and mechanisms of flavonoids on cancer prevention and therapy: focus on gut microbiota. *Int J Biol Sci*. 2022;18:1451-1475. doi:10.7150/ijbs.68170
81. Alghetaa H, Mohammed A, Zhou J, et al. Resveratrol-mediated attenuation of superantigen-driven acute respiratory distress syndrome is mediated by microbiota in the lungs and gut. *Pharmacol Res*. 2021;167:105548. doi:10.1016/j.phrs.2021.105548
82. Hartmann N, Kronenberg M. Cancer immunity thwarted by the microbiome. *Science*. 2018;360:858-859. doi:10.1126/science.aat8289
83. Hang S, Paik D, Yao L, et al. Bile acid metabolites control T(H)17 and T(reg) cell differentiation. *Nature*. 2019;576:143-148. doi:10.1038/s41586-019-1785-z
84. Paik D, Yao L, Zhang Y, et al. Human gut bacteria produce T(H)17-modulating bile acid metabolites. *Nature*. 2022;603:907-912. doi:10.1038/s41586-022-04480-z
85. Vujkovic-Cvijin I, Sklar J, Jiang L, et al. Host variables confound gut microbiota studies of human disease. *Nature*. 2020;587:448-454. doi:10.1038/s41586-020-2881-9